PHYSICAL REVIEW D **87,** 112004 (2013)

Study of $J/\psi \to \omega p \bar{p}$ at BESIII

M. Ablikim,[1] M. N. Achasov,[6] O. Albayrak,[3] D. J. Ambrose,[39] F. F. An,[1] Q. An,[40] J. Z. Bai,[1] R. Baldini Ferroli,[17a] Y. Ban,[26] J. Becker,[2] J. V. Bennett,[16] M. Bertani,[17a] J. M. Bian,[38] E. Boger,[19,*] O. Bondarenko,[20] I. Boyko,[19] R. A. Briere,[3] V. Bytev,[19] H. Cai,[44] X. Cai,[1] O. Cakir,[34a] A. Calcaterra,[17a] G. F. Cao,[1] S. A. Cetin,[34b] J. F. Chang,[1] G. Chelkov,[19,*] G. Chen,[1] H. S. Chen,[1] J. C. Chen,[1] M. L. Chen,[1] S. J. Chen,[24] X. Chen,[26] Y. Chen,[1] Y. B. Chen,[1] H. P. Cheng,[14] Y. P. Chu,[1] D. Cronin-Hennessy,[38] H. L. Dai,[1] J. P. Dai,[1] D. Dedovich,[19] Z. Y. Deng,[1] A. Denig,[18] I. Denysenko,[19,†] M. Destefanis,[43a,43c] W. M. Ding,[28] Y. Ding,[22] L. Y. Dong,[1] M. Y. Dong,[1] S. X. Du,[46] J. Fang,[1] S. S. Fang,[1] L. Fava,[43b,43c] C. Q. Feng,[40] P. Friedel,[2] C. D. Fu,[1] J. L. Fu,[24] O. Fuks,[19,*] Y. Gao,[33] C. Geng,[40] K. Goetzen,[7] W. X. Gong,[1] W. Gradl,[18] M. Greco,[43a,43c] M. H. Gu,[1] Y. T. Gu,[9] Y. H. Guan,[36] A. Q. Guo,[25] L. B. Guo,[23] T. Guo,[23] Y. P. Guo,[25] Y. L. Han,[1] F. A. Harris,[37] K. L. He,[1] M. He,[1] Z. Y. He,[25] T. Held,[2] Y. K. Heng,[1] Z. L. Hou,[1] C. Hu,[23] H. M. Hu,[1] J. F. Hu,[35] T. Hu,[1] G. M. Huang,[4] G. S. Huang,[40] J. S. Huang,[12] L. Huang,[1] X. T. Huang,[28] Y. Huang,[24] Y. P. Huang,[1] T. Hussain,[42] C. S. Ji,[40] Q. Ji,[1] Q. P. Ji,[25] X. B. Ji,[1] X. L. Ji,[1] L. L. Jiang,[1] X. S. Jiang,[1] J. B. Jiao,[28] Z. Jiao,[14] D. P. Jin,[1] S. Jin,[1] F. F. Jing,[33] N. Kalantar-Nayestanaki,[20] M. Kavatsyuk,[20] B. Kopf,[2] M. Kornicer,[37] W. Kuehn,[35] W. Lai,[1] J. S. Lange,[35] P. Larin,[11] M. Leyhe,[2] C. H. Li,[1] Cheng Li,[40] Cui Li,[40] D. M. Li,[46] F. Li,[1] G. Li,[1] H. B. Li,[1] J. C. Li,[1] K. Li,[10] Lei Li,[1] Q. J. Li,[1] S. L. Li,[1] W. D. Li,[1] W. G. Li,[1] X. L. Li,[28] X. N. Li,[1] X. Q. Li,[25] X. R. Li,[27] Z. B. Li,[32] H. Liang,[40] Y. F. Liang,[30] Y. T. Liang,[35] G. R. Liao,[33] X. T. Liao,[1] D. Lin,[11] B. J. Liu,[1] C. L. Liu,[3] C. X. Liu,[1] F. H. Liu,[29] Fang Liu,[1] Feng Liu,[4] H. Liu,[1] H. B. Liu,[9] H. H. Liu,[13] H. M. Liu,[1] H. W. Liu,[1] J. P. Liu,[44] K. Liu,[33] K. Y. Liu,[22] Kai Liu,[36] P. L. Liu,[28] Q. Liu,[36] S. B. Liu,[40] X. Liu,[21] Y. B. Liu,[25] Z. A. Liu,[1] Zhiqiang Liu,[1] Zhiqing Liu,[1] H. Loehner,[20] G. R. Lu,[12] H. J. Lu,[14] J. G. Lu,[1] Q. W. Lu,[29] X. R. Lu,[36] Y. P. Lu,[1] C. L. Luo,[23] M. X. Luo,[45] T. Luo,[37] X. L. Luo,[1] M. Lv,[1] C. L. Ma,[36] F. C. Ma,[22] H. L. Ma,[1] Q. M. Ma,[1] S. Ma,[1] T. Ma,[1] X. Y. Ma,[1] F. E. Maas,[11] M. Maggiora,[43a,43c] Q. A. Malik,[42] Y. J. Mao,[26] Z. P. Mao,[1] J. G. Messchendorp,[20] J. Min,[1] T. J. Min,[1] R. E. Mitchell,[16] X. H. Mo,[1] H. Moeini,[20] C. Morales Morales,[11] K. Moriya,[16] N. Yu. Muchnoi,[6] H. Muramatsu,[39] Y. Nefedov,[19] C. Nicholson,[36] I. B. Nikolaev,[6] Z. Ning,[1] S. L. Olsen,[27] Q. Ouyang,[1] S. Pacetti,[17b] J. W. Park,[27] M. Pelizaeus,[2] H. P. Peng,[40] K. Peters,[7] J. L. Ping,[23] R. G. Ping,[1] R. Poling,[38] E. Prencipe,[18] M. Qi,[24] S. Qian,[1] C. F. Qiao,[36] L. Q. Qin,[28] X. S. Qin,[1] Y. Qin,[26] Z. H. Qin,[1] J. F. Qiu,[1] K. H. Rashid,[42] G. Rong,[1] X. D. Ruan,[9] A. Sarantsev,[19,‡] B. D. Schaefer,[16] M. Shao,[40] C. P. Shen,[37,§] X. Y. Shen,[1] H. Y. Sheng,[1] M. R. Shepherd,[16] W. M. Song,[1] X. Y. Song,[1] S. Spataro,[43a,43c] B. Spruck,[35] D. H. Sun,[1] G. X. Sun,[1] J. F. Sun,[12] S. S. Sun,[1] Y. J. Sun,[40] Y. Z. Sun,[1] Z. J. Sun,[1] Z. T. Sun,[40] C. J. Tang,[30] X. Tang,[1] I. Tapan,[34c] E. H. Thorndike,[39] D. Toth,[38] M. Ullrich,[35] I. Uman,[34b] G. S. Varner,[37] B. Q. Wang,[26] D. Wang,[26] D. Y. Wang,[26] K. Wang,[1] L. L. Wang,[1] L. S. Wang,[1] M. Wang,[28] P. Wang,[1] P. L. Wang,[1] Q. J. Wang,[1] S. G. Wang,[26] X. F. Wang,[33] X. L. Wang,[40] Y. D. Wang,[17a] Y. F. Wang,[1] Y. Q. Wang,[18] Z. Wang,[1] Z. G. Wang,[1] Z. Y. Wang,[1] D. H. Wei,[8] J. B. Wei,[26] P. Weidenkaff,[18] Q. G. Wen,[40] S. P. Wen,[1] M. Werner,[35] U. Wiedner,[2] L. H. Wu,[1] N. Wu,[1] S. X. Wu,[40] W. Wu,[25] Z. Wu,[1] L. G. Xia,[33] Y. X. Xia,[15] Z. J. Xiao,[23] Y. G. Xie,[1] Q. L. Xiu,[1] G. F. Xu,[1] G. M. Xu,[26] Q. J. Xu,[10] Q. N. Xu,[36] X. P. Xu,[31] Z. R. Xu,[40] F. Xue,[4] Z. Xue,[1] L. Yan,[40] W. B. Yan,[40] Y. H. Yan,[15] H. X. Yang,[1] Y. Yang,[4] Y. X. Yang,[8] H. Ye,[1] M. Ye,[1] M. H. Ye,[5] B. X. Yu,[1] C. X. Yu,[25] H. W. Yu,[26] J. S. Yu,[21] S. P. Yu,[28] C. Z. Yuan,[1] Y. Yuan,[1] A. A. Zafar,[42] A. Zallo,[17a] S. L. Zang,[24] Y. Zeng,[15] B. X. Zhang,[1] B. Y. Zhang,[1] C. Zhang,[24] C. C. Zhang,[1] D. H. Zhang,[1] H. H. Zhang,[32] H. Y. Zhang,[1] J. Q. Zhang,[1] J. W. Zhang,[1] J. Y. Zhang,[1] J. Z. Zhang,[1] LiLi Zhang,[15] R. Zhang,[36] S. H. Zhang,[1] X. J. Zhang,[1] X. Y. Zhang,[28] Y. Zhang,[1] Y. H. Zhang,[1] Z. P. Zhang,[40] Z. Y. Zhang,[44] Zhenghao Zhang,[4] G. Zhao,[1] H. S. Zhao,[1] J. W. Zhao,[1] K. X. Zhao,[23] Lei Zhao,[40] Ling Zhao,[1] M. G. Zhao,[25] Q. Zhao,[1] S. J. Zhao,[46] T. C. Zhao,[1] X. H. Zhao,[24] Y. B. Zhao,[1] Z. G. Zhao,[40] A. Zhemchugov,[19,*] B. Zheng,[41] J. P. Zheng,[1] Y. H. Zheng,[36] B. Zhong,[23] L. Zhou,[1] X. Zhou,[44] X. K. Zhou,[36] X. R. Zhou,[40] C. Zhu,[1] K. Zhu,[1] K. J. Zhu,[1] S. H. Zhu,[1] X. L. Zhu,[33] Y. C. Zhu,[40] Y. M. Zhu,[25] Y. S. Zhu,[1] Z. A. Zhu,[1] J. Zhuang,[1] B. S. Zou,[1] and J. H. Zou[1]

(BESIII Collaboration)

[1]*Institute of High Energy Physics, Beijing 100049, People's Republic of China*
[2]*Bochum Ruhr-University, D-44780 Bochum, Germany*
[3]*Carnegie Mellon University, Pittsburgh, Pennsylvania 15213, USA*
[4]*Central China Normal University, Wuhan 430079, People's Republic of China*
[5]*China Center of Advanced Science and Technology, Beijing 100190, People's Republic of China*
[6]*G.I. Budker Institute of Nuclear Physics SB RAS (BINP), Novosibirsk 630090, Russia*
[7]*GSI Helmholtzcentre for Heavy Ion Research GmbH, D-64291 Darmstadt, Germany*
[8]*Guangxi Normal University, Guilin 541004, People's Republic of China*
[9]*GuangXi University, Nanning 530004, People's Republic of China*

 © 2013 American Physical Society

[10]*Hangzhou Normal University, Hangzhou 310036, People's Republic of China*
[11]*Helmholtz Institute Mainz, Johann-Joachim-Becher-Weg 45, D-55099 Mainz, Germany*
[12]*Henan Normal University, Xinxiang 453007, People's Republic of China*
[13]*Henan University of Science and Technology, Luoyang 471003, People's Republic of China*
[14]*Huangshan College, Huangshan 245000, People's Republic of China*
[15]*Hunan University, Changsha 410082, People's Republic of China*
[16]*Indiana University, Bloomington, Indiana 47405, USA*
[17a]*INFN Laboratori Nazionali di Frascati, I-00044 Frascati, Italy*
[17b]*INFN and University of Perugia, I-06100 Perugia, Italy*
[18]*Johannes Gutenberg University of Mainz, Johann-Joachim-Becher-Weg 45, D-55099 Mainz, Germany*
[19]*Joint Institute for Nuclear Research, 141980 Dubna, Moscow region, Russia*
[20]*KVI, University of Groningen, NL-9747 AA Groningen, The Netherlands*
[21]*Lanzhou University, Lanzhou 730000, People's Republic of China*
[22]*Liaoning University, Shenyang 110036, People's Republic of China*
[23]*Nanjing Normal University, Nanjing 210023, People's Republic of China*
[24]*Nanjing University, Nanjing 210093, People's Republic of China*
[25]*Nankai University, Tianjin 300071, People's Republic of China*
[26]*Peking University, Beijing 100871, People's Republic of China*
[27]*Seoul National University, Seoul 151-747, Korea*
[28]*Shandong University, Jinan 250100, People's Republic of China*
[29]*Shanxi University, Taiyuan 030006, People's Republic of China*
[30]*Sichuan University, Chengdu 610064, People's Republic of China*
[31]*Soochow University, Suzhou 215006, People's Republic of China*
[32]*Sun Yat-Sen University, Guangzhou 510275, People's Republic of China*
[33]*Tsinghua University, Beijing 100084, People's Republic of China*
[34a]*Ankara University, Dogol Caddesi, 06100 Tandogan, Ankara, Turkey*
[34b]*Dogus University, 34722 Istanbul, Turkey*
[34c]*Uludag University, 16059 Bursa, Turkey*
[35]*Universitaet Giessen, D-35392 Giessen, Germany*
[36]*University of Chinese Academy of Sciences, Beijing 100049, People's Republic of China*
[37]*University of Hawaii, Honolulu, Hawaii 96822, USA*
[38]*University of Minnesota, Minneapolis, Minnesota 55455, USA*
[39]*University of Rochester, Rochester, New York 14627, USA*
[40]*University of Science and Technology of China, Hefei 230026, People's Republic of China*
[41]*University of South China, Hengyang 421001, People's Republic of China*
[42]*University of the Punjab, Lahore 54590, Pakistan*
[43a]*University of Turin, I-10125 Turin, Italy*
[43b]*University of Eastern Piedmont, I-15121 Alessandria, Italy*
[43c]*INFN, I-10125 Turin, Italy*
[44]*Wuhan University, Wuhan 430072, People's Republic of China*
[45]*Zhejiang University, Hangzhou 310027, People's Republic of China*
[46]*Zhengzhou University, Zhengzhou 450001, People's Republic of China*

(Received 14 March 2013; published 3 June 2013)

The decay $J/\psi \to \omega p\bar{p}$ has been studied, using 225.3×10^6 J/ψ events accumulated at BESIII. No significant enhancement near the $p\bar{p}$ invariant-mass threshold [denoted as $X(p\bar{p})$] is observed. The upper limit of the branching fraction $\mathcal{B}(J/\psi \to \omega X(p\bar{p}) \to \omega p\bar{p})$ is determined to be 3.9×10^{-6} at the 95% confidence level. The branching fraction of $J/\psi \to \omega p\bar{p}$ is measured to be $\mathcal{B}(J/\psi \to \omega p\bar{p}) = (9.0 \pm 0.2(\text{stat}) \pm 0.9(\text{syst})) \times 10^{-4}$.

DOI: 10.1103/PhysRevD.87.112004 PACS numbers: 13.25.Gv, 12.39.Mk, 13.75.Cs

I. INTRODUCTION

An anomalous enhancement near the threshold of the $p\bar{p}$ system, namely $X(p\bar{p})$, was first observed by the BESII experiment in the radiative decay $J/\psi \to \gamma p\bar{p}$ [1], and it was recently confirmed by the CLEO and BESIII experiments [2–4]. In the BESII experiment, its mass is measured

*Also at the Moscow Institute of Physics and Technology, Moscow 141700, Russia.
†On leave from the Bogolyubov Institute for Theoretical Physics, Kiev 03680, Ukraine.
‡Also at the PNPI, Gatchina 188300, Russia.
§Present address: Nagoya University, Nagoya 464-8601, Japan.

to be $1859^{+3}_{-10}(\text{stat})^{+5}_{-25}(\text{syst})$ MeV/c^2 and the total width is $\Gamma < 30$ MeV/c^2 at the 90% confidence level (C.L.). While in the BESIII experiment, a partial wave analysis with a correction for the final-state interaction (FSI) is performed, and the spin parity of $X(p\bar{p})$ is determined to be 0^{-+}, its mass is $1832^{+19}_{-5}(\text{stat})^{+18}_{-17}(\text{syst})$ MeV/c^2 and the total width is $\Gamma < 76$ MeV/c^2 at the 90% C.L. [3].

The discovery of $X(p\bar{p})$ stimulated a number of theoretical interpretations and experimental studies [5–16]. There is no experimental evidence of such an enhancement in other quarkonium decays, e.g., $J/\psi \to \pi^0 p\bar{p}$ [1] or $\Upsilon(2S) \to \gamma p\bar{p}$ [5]. In $\psi(2S) \to \gamma p\bar{p}$, the recent BESIII measurement shows a relative production rate to that of J/ψ decays of $R = 5.08\%$ [3]. A number of theoretical speculations have been proposed to interpret the nature of this structure, including baryonium [9–11], a multiquark state [12] or mainly a pure FSI [13,14]. It was proposed to associate this enhancement with a broad enhancement observed in B meson decays [17,18] or a new resonance $X(1835)$ in $J/\psi \to \gamma\pi^+\pi^-\eta'$ decay at BESII [19].

The investigation of the near-threshold $p\bar{p}$ invariant mass spectrum in other J/ψ decay modes will be helpful in understanding the nature of the observed structure. The decay $J/\psi \to \omega p\bar{p}$ restricts the isospin of the $p\bar{p}$ system, and it is helpful to clarify the role of the $p\bar{p}$ FSI. The BESII Collaboration studied $J/\psi \to \omega p\bar{p}$ via ω decaying to $\pi^0\pi^+\pi^-$ with a data sample of 5.8×10^7 J/ψ events [6]. No significant signal near the threshold of the $p\bar{p}$ invariant-mass spectrum was observed, and an upper limit on the branching fraction of $J/\psi \to \omega X(p\bar{p}) \to \omega p\bar{p}$ was determined to be 1.5×10^{-5} at the 90% C.L., which disfavored the interpretation of a pure FSI effect giving rise to the $X(p\bar{p})$. In this paper, the analysis of $J/\psi \to \omega p\bar{p}$ via the decay channel $\omega \to \gamma\pi^0$ is presented, based on a data sample of $(225.3 \pm 2.8) \times 10^6$ J/ψ events [20] accumulated with the BESIII detector. Searching for the $X(p\bar{p})$ in the decay mode $J/\psi \to \omega p\bar{p} \to \gamma\pi^0 p\bar{p}$ has a particular advantage: a low irreducible background from N^* is expected. The channel $J/\psi \to \omega p\bar{p} \to \pi\pi\pi^0 p\bar{p}$ has irreducible background from various N^* decays and Δ decays, where interferences may have a large impact on the uncertainty of the measurements.

BESIII/BEPCII [21] is a major upgrade of the BESII experiment at the BEPC accelerator [22] for studies of hadron spectroscopy and τ-charm physics [23]. The design peak luminosity of the double-ring e^+e^- collider, BEPCII, is 10^{33} cm^{-2} s^{-1} at beam currents of 0.93 A. The BESIII detector with a geometrical acceptance of 93% of 4π consists of the following main components: (1) a small-celled, helium-based main drift chamber with 43 layers (the average single wire resolution is 135 μm, and the momentum resolution for 1 GeV/c^2 charged particles in a 1 T magnetic field is 0.5%); (2) an electromagnetic calorimeter (EMC) made of 6240 CsI (Tl) crystals arranged in a cylindrical shape (barrel) plus two end caps (for 1.0 GeV photons, the energy resolution is 2.5% in the barrel and 5% in the end caps, and the position resolution is 6 mm in the barrel and 9 mm in the end caps); (3) a time-of-flight system for particle identification (PID) composed of a barrel part made of two layers with 88 pieces of 5 cm thick, 2.4 m long plastic scintillators in each layer, and two end caps with 48 fan-shaped, 5 cm thick, plastic scintillators in each end cap (the time resolution is 80 ps in the barrel and 110 ps in the end caps, corresponding to a K/π separation by more than 2σ for momenta below about 1 GeV/c^2); (4) a muon chamber system made of 1000 m^2 of resistive plate chambers arranged in nine layers in the barrel and eight layers in the end caps and incorporated in the return iron yoke of the superconducting magnet. The position resolution is about 2 cm.

The optimization of the event selection and the estimate of physics backgrounds are performed through Monte Carlo (MC) simulations. The GEANT4-based simulation software BOOST [24] includes the geometric and material description of the BESIII detectors and the detector response and digitization models, as well as the tracking of the detector running conditions and performance. The production of the J/ψ resonance is simulated by the MC event generator KKMC [25], while the decays are generated by EVTGEN [26] for known decay modes with branching ratios being set to Particle Data Group (PDG) [27] world average values, and by LUNDCHARM [28] for the remaining unknown decays. The analysis is performed in the framework of the BESIII offline software system [29] which takes care of the detector calibration, event reconstruction and data storage.

II. EVENT SELECTION

Signal $J/\psi \to \omega p\bar{p}$ events with $\omega \to \gamma\pi^0$ final states have the topology $\gamma\gamma\gamma p\bar{p}$. The event candidates are required to have two well-reconstructed charged tracks with net charge zero, and at least three photons.

Charged-particle tracks in the polar angle range $|\cos\theta| < 0.93$ are reconstructed from the main drift chamber hits; only tracks in the barrel region ($|\cos\theta| < 0.8$) are used to reduce systematic uncertainties in tracking and particle identification. Tracks with their points of closest approach to the beamline within ± 10 cm of the interaction point in the beam direction and within 1 cm in the plane perpendicular to the beam are selected. time-of-flight system and $\mathrm{d}E/\mathrm{d}x$ information are combined to determine particle identification confidence levels for π, K and $p(\bar{p})$ hypotheses; and the particle type with the highest confidence level is assigned to each track. A proton and an antiproton are required. To reduce the systematic error due to differences of the tracking efficiency at low momentum between data and MC, the momentum of the proton or antiproton is further required to be larger than 300 MeV/c.

Photon candidates are reconstructed by clustering signals in EMC crystals. The photon candidates are required

to be in the barrel region ($|\cos\theta| < 0.8$) of the EMC with at least 25 MeV energy deposition, or in the end-cap region ($0.86 < |\cos\theta| < 0.92$) with at least 50 MeV energy deposition, where θ is the polar angle of the shower. Timing information from the EMC is used to suppress electronic noise and energy depositions that are unrelated to the event. To suppress showers generated by charged particles, the photon candidates are furthermore required to be separated by an angle larger than 10° and larger than 30° from the proton and antiproton, respectively.

A four-constraint (4C) energy-momentum conserving kinematic fit is performed on the $\gamma\gamma\gamma p\bar{p}$ hypothesis. For events with more than three photon candidates, the combination with the minimum χ^2_{4C} is selected, and $\chi^2_{4C} < 30$ is required. The π^0 candidates are reconstructed from the two of the three selected photons with an invariant mass closest to the π^0 mass, and $|M_{\gamma\gamma} - M_{\pi^0}| < 15$ MeV/c^2 is required.

III. BRANCHING FRACTION AND YIELD MEASUREMENTS

Figure 1 shows the $\gamma\pi^0$ invariant mass spectrum for candidate $J/\psi \to \gamma\pi^0 p\bar{p}$ events, where a distinctive ω signal is seen. An unbinned maximum likelihood fit is performed on the $\gamma\pi^0$ invariant mass with the ω signal parametrized by a Breit-Wigner function convoluted with the Novosibirsk function [30] which describes the detector resolution. The background shape is described by a second-order Chebychev polynomial function. The mass and width of the ω peak are fixed to the values published by

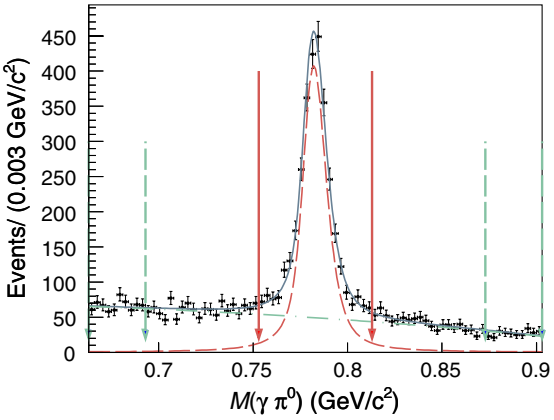

FIG. 1 (color online). $\gamma\pi^0$ invariant mass distribution of $J/\psi \to \gamma\pi^0 p\bar{p}$ candidates. The dashed line is the signal shape which is parametrized by a Breit-Wigner function convoluted with the detector resolution described by the Novosibirsk function; the dashed-dotted line is the background shape which is described by a second order Chebychev polynomial; and the solid line is the total contribution of the two components. The solid arrows indicate the ω signal region [$0.753 < M(\gamma\pi^0) < 0.813$ GeV/c^2] and the two pairs of dashed arrows indicate the ω sidebands [$0.663 < M(\gamma\pi^0) < 0.693$ GeV/c^2 and $0.873 < M(\gamma\pi^0) < 0.903$ GeV/c^2].

the PDG [27], and the yield of the ω signal obtained from the fit is $N_{\rm obs} = 2670 \pm 69$.

The branching fraction of $J/\psi \to \omega p\bar{p}$ is calculated according to

$$\mathcal{B}(J/\psi \to \omega p\bar{p}) = \frac{N_{\rm obs}}{N_{J/\psi} \times \mathcal{B}(\omega \to \gamma\pi^0) \times \mathcal{B}(\pi^0 \to \gamma\gamma) \times \varepsilon_{\rm rec}}, \quad (1)$$

where $N_{\rm obs}$ is the number of signal events determined from the fit to the $\gamma\pi^0$ invariant mass; $N_{J/\psi}$ is the number of J/ψ events [20]; $\mathcal{B}(\omega \to \gamma\pi^0)$ and $\mathcal{B}(\pi^0 \to \gamma\gamma)$ are branching fractions of $\omega \to \gamma\pi^0$ and $\pi^0 \to \gamma\gamma$, respectively, as from the PDG [27]; and the detection efficiency $\varepsilon_{\rm rec}$ is $(16.1 \pm 1.7)\%$ obtained from a MC sample for $J/\psi \to \omega p\bar{p}$ events generated according to a phase-space distribution. The measured branching fraction is $\mathcal{B}(J/\psi \to \omega p\bar{p}) = (9.0 \pm 0.2(\text{stat})) \times 10^{-4}$.

Candidate $J/\psi \to \omega p\bar{p}$ events are selected with the mass window requirement 0.753 GeV/$c^2 < M(\gamma\pi^0) <$ 0.813 GeV/c^2, and the Dalitz plot of these events is shown in Fig. 2. There are no obvious structures in the Dalitz plot, though the distribution is different from the pure $\omega p\bar{p}$ phase-space distribution. The corresponding $p\bar{p}$, ωp and $\omega\bar{p}$ invariant-mass spectra are also presented in Fig. 2. The data points with error bars are from the signal region and the hatched area is from the sideband region. The mass threshold is shown in Fig. 3.

To obtain the number of $J/\psi \to \omega X(p\bar{p}) \to \omega p\bar{p}$ events, an unbinned maximum likelihood fit is performed on the $p\bar{p}$ invariant mass around the mass threshold. In the fit, the spin parity of $X(p\bar{p})$ is assumed to be 0^-, and the signal of $X(p\bar{p})$ in the $J/\psi \to \omega X(p\bar{p}) \to \omega p\bar{p}$ decay is parametrized by an acceptance-weighted $\mathcal{S}$-wave Breit-Wigner function:

$$\text{BW}(M) \simeq \frac{q^{2L+1}k^3}{(M^2 - M_0^2)^2 + M_0^2\Gamma^2} \times \varepsilon_{\rm rec}(M). \quad (2)$$

Here, q is the momentum of the proton in the $p\bar{p}$ rest frame; k is the momentum of the ω meson; $L = 0$ is the relative orbital angular momentum; M is the invariant mass of $p\bar{p}$; M_0 and Γ are the mass and width of the $X(p\bar{p})$, respectively, which are taken from BESIII results [3]; $\varepsilon_{\rm rec}$ is the detection efficiency. The non-ω background is presented by a function of the form $f(\delta) = N(\delta^{1/2} + a_1\delta^{3/2} + a_2\delta^{5/2})$ with $\delta = M_{p\bar{p}} - 2m_p$ where m_p is the proton mass. The normalization and shape parameters a_1 and a_2 are determined by a simultaneous fit to the $M(p\bar{p})$ in the ω signal region and the ω sideband region 0.09 GeV/$c^2 < |M(\gamma\pi^0) - 0.783| < 0.12$ GeV/c^2. The nonresonant $J/\psi \to \omega p\bar{p}$ events are also described by the function $f(\delta)$, where the normalization and shape parameters are allowed to float. The fit results are shown in Fig. 3, and the number of $X(p\bar{p})$ events is 0 ± 1.6. A Bayesian approach [27] estimates the upper limit of

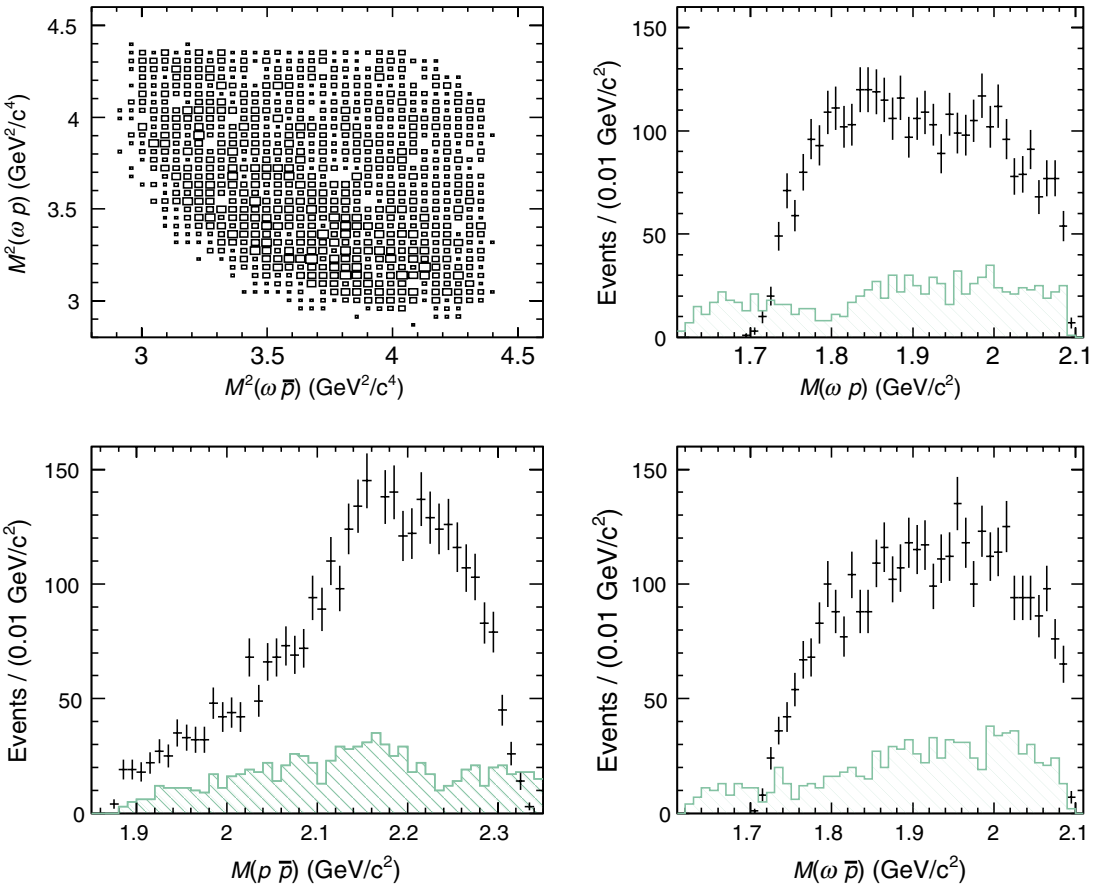

FIG. 2 (color online). Dalitz plot and $p\bar{p}$, ωp, $\omega\bar{p}$ invariant-mass spectra of $J/\psi \to \omega p\bar{p}$ candidates. The data points with error bars are from the signal region and the hatched areas are from the sideband region.

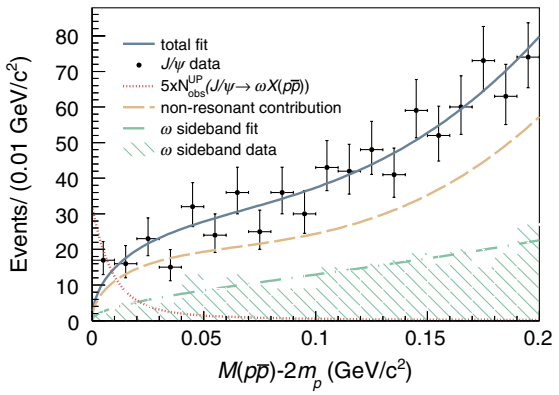

FIG. 3 (color online). Near-threshold $p\bar{p}$ invariant-mass spectrum. The signal $J/\psi \to \omega X(p\bar{p}) \to \omega p\bar{p}$ is described by an acceptance-weighted Breit-Wigner function, and the signal yield is consistent with zero. The dotted line is the shape of the signal which is normalized to 5 times the estimated upper limit. The dashed line is the nonresonant contribution described by the function $f(\delta)$ and the dashed-dotted line is the non-$\omega p\bar{p}$ contribution which is estimated from ω sidebands. The solid line is the total contribution of the two components. The hatched area is from the sideband region.

$\mathcal{B}(J/\psi \to \omega X(p\bar{p}) \to \omega p\bar{p})$, and $N_{\rm obs} < 9$ at 95% C. L. is determined by finding the value $N^{\rm UP}_{\rm obs}$ with

$$\frac{\int_0^{N^{\rm UP}_{\rm obs}} \mathcal{L} dN_{\rm obs}}{\int_0^{\infty} \mathcal{L} dN_{\rm obs}} = 0.95, \tag{3}$$

where $N_{\rm obs}$ is the number of signal events, and $\mathcal{L}$ is the value of the likelihood function with the $N_{\rm obs}$ value fixed in the fit. The upper limit on the product of branching fractions is calculated with

$$\mathcal{B}(J/\psi \to \omega X(p\bar{p}) \to \omega p\bar{p}) < \frac{N^{\rm UL}_{\rm obs}}{N_{J/\psi} \times (1-\sigma_{\rm sys}) \times \mathcal{B}(\omega \to \gamma\pi^0) \times \mathcal{B}(\pi^0 \to \gamma\gamma) \times \varepsilon_{\rm rec}}, \tag{4}$$

where $\sigma_{\rm sys}$ is the total systematic uncertainty which will be described in the next section. The upper limit on the product of branching fractions is $\mathcal{B}(J/\psi \to \omega X(p\bar{p}) \to \omega p\bar{p}) < 3.9 \times 10^{-6}$ at the 95% C.L.

An alternative fit with a Breit-Wigner function including the Jülich FSI

$$\mathrm{BW}(M) \simeq \frac{f_{\mathrm{FSI}} \times q^{2L+1}k^3}{(M^2 - M_0^2)^2 + M_0^2\Gamma^2} \times \varepsilon_{\mathrm{rec}}(M), \quad (5)$$

for $X(p\bar{p})$, is performed. Here, f_{FSI} is the Jülich FSI correction factor [14]. The mass and width of $X(p\bar{p})$ are taken from the previous BESIII partial wave analysis results [3]. The upper limit on the product of branching fractions is determined to be $\mathcal{B}(J/\psi \to \omega X(p\bar{p}) \to \omega p\bar{p}) < 3.7 \times 10^{-6}$ at the 95% C.L.

IV. SYSTEMATIC UNCERTAINTIES

Several sources of systematic uncertainties are considered in the measurement of the branching fractions. These include differences between data and the MC simulation for the tracking algorithm, the PID, photon detection, the kinematic fit, as well as the fitting procedure, the branching fraction of the intermediate states and the total number of J/ψ events. The systematic uncertainties of $\mathcal{B}(J/\psi \to \omega p\bar{p})$ and the upper limit of $\mathcal{B}(J/\psi \to \omega X(p\bar{p}) \to \omega p\bar{p})$ are summarized in Table I.

The systematic uncertainties associated with the tracking efficiency and PID efficiency have been studied with $J/\psi \to p\bar{p}\pi^+\pi^-$ using a technique similar to that discussed in Ref. [31]. The difference of tracking efficiencies between data and MC simulation is 2% per charged track. The systematic uncertainty from PID is 2% per proton (antiproton).

The photon detection systematic uncertainty is studied by comparing the photon efficiency between MC simulation and the control sample $J/\psi \to \rho\pi$. The relative efficiency difference is about 1% for each photon [32,33]. Here, 3% is taken as the systematic error for the efficiency of detecting three photons. The uncertainty due to π^0 reconstruction efficiency is taken as 1% [32,33].

To estimate the uncertainty associated with the kinematic fit, selected samples of $J/\psi \to \Sigma^+\bar{\Sigma}^- \to p\pi^0\bar{p}\pi^0$ events are used. The kinematic fit efficiency is defined as the ratio between the signal yield of Σ^+ with or without the kinematic fit. The difference of kinematic fit efficiency between data and MC is 3% and is taken as the systematic uncertainty caused by the kinematic fit.

As described above, the yield of $J/\psi \to \omega p\bar{p}$ is derived from a fit to the invariant-mass spectrum of $\gamma\pi^0$ pairs. To evaluate the systematic uncertainty associated with the fitting procedure, the following two aspects are studied. (i) *Fitting region*: In the nominal fit, the mass spectrum of $\gamma\pi^0$ is fitted in the range from 0.663 GeV/c^2 to 0.903 GeV/c^2. Alternative fits within the ranges 0.653 GeV/c^2 to 0.913 GeV/c^2 and 0.673 GeV/c^2 to 0.893 GeV/c^2 are performed, and the difference in the signal yield of 2% is taken as the systematic uncertainty associated with the fit interval. (ii) *Background shape*: To estimate the uncertainty due to the background parametrization for the branching fraction $\mathcal{B}(J/\psi \to \omega p\bar{p})$, a first- or third-order instead of a second-order Chebychev polynomial is used in the fitting. The difference of 1.2% is used as an estimate of the systematic uncertainty.

For the upper limit on the branching fraction $\mathcal{B}(J/\psi \to \omega X(p\bar{p}) \to \omega p\bar{p})$, the systematic uncertainty associated with the fitting procedure is estimated by fixing the shape of the nonresonant contribution to a phase-space MC simulation of $J/\psi \to \omega p\bar{p}$, which is presented in Fig. 4; enlarging or reducing the normalization of the non-ω contribution by 7% (the difference of the estimation of the non-ω background level between data and inclusive MC); and varying the sideband region to 0.095 GeV/c^2 < $|M(\gamma\pi^0) - 0.783| < 0.115$ GeV/c^2 and 0.085 GeV/c^2 < $|M(\gamma\pi^0) - 0.783| < 0.125$ GeV/c^2. When fitting with or without the FSI effect, the signal yields for the alternative fits are lower than or equal to the nominal fit; therefore, the conservative upper limit from the fit without the FSI correction is reported.

Various distributions obtained with data and the phase-space MC sample have been compared, and some discrepancies are observed. To determine the systematic

TABLE I. Summary of systematic uncertainties. The "···" means the corresponding systematic uncertainty is negligible.

Source	$\mathcal{B}(J/\psi \to \omega p\bar{p})$	Upper limit of $\mathcal{B}(J/\psi \to \omega X(p\bar{p}) \to \omega p\bar{p})$	Upper limit of $\mathcal{B}(J/\psi \to \omega X(p\bar{p}) \to \omega p\bar{p})$ with FSI
Tracking	4%	4%	4%
PID	4%	4%	4%
Photon	3%	3%	3%
Kinematic fit	3%	3%	3%
π^0 reconstruction	1%	1%	1%
Fitting region	2%	···	···
Background shape	1%	···	···
Branching fraction of intermediate state	3%	3%	3%
Total J/ψ numbers	1.24%	1.24%	1.24%
MC generator	7%	···	···
Total uncertainty	10.3%	7.8%	7.8%

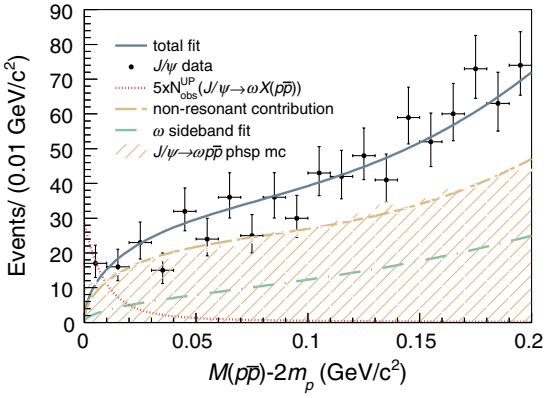

FIG. 4 (color online). Near-threshold $p\bar{p}$ invariant-mass spectrum. The signal $J/\psi \to \omega X(p\bar{p}) \to \omega p\bar{p}$ is described by an acceptance-weighted Breit-Wigner function, and the signal yield is consistent with zero. The dashed line is the nonresonant contribution fixed to a phase-space MC simulation of $J/\psi \to \omega p\bar{p}$ and the dashed-dotted line is the non-$\omega p\bar{p}$ contribution which is estimated from ω sidebands. The solid line is the total contribution of the two components. The hatched area is from a phase-space MC simulation of $J/\psi \to \omega p\bar{p}$.

error on the detection efficiency associated with these discrepancies, an alternative detection efficiency is estimated by reweighting phase-space MC samples. The difference in detection efficiency compared to the nominal one is 7% and taken as a systematic uncertainty. The number of J/ψ events is determined from an inclusive analysis of J/ψ hadronic events, and an uncertainty of 1.24% is associated to it [20]. The uncertainties due to the branching fractions of $\omega \to \gamma\pi^0$ and $\pi^0 \to \gamma\gamma$ are taken from the PDG [27].

V. SUMMARY

In summary, using $(225.3 \pm 2.8) \times 10^6$ J/ψ events collected with the BESIII detector, the decay of $J/\psi \to \omega p\bar{p}$ in the decay mode $\omega \to \gamma\pi^0$ is studied. The branching fraction $\mathcal{B}(J/\psi \to \omega p\bar{p})$ is measured to be $(9.0 \pm 0.2(\text{stat}) \pm 0.9(\text{syst})) \times 10^{-4}$. No obvious enhancement around the $p\bar{p}$ invariant-mass threshold is observed. At the 95% C.L., the upper limits on the product of branching fractions $\mathcal{B}(J/\psi \to \omega X(p\bar{p}) \to \omega p\bar{p})$ are measured to be 3.7×10^{-6} and 3.9×10^{-6} with and without accounting for the Jülich FSI effect, respectively. As the isospins for $J/\psi \to \gamma p\bar{p}$ and $\omega p\bar{p}$ should both favor $I = 0$ ($I = 1$ should be suppressed in $J/\psi \to \gamma p\bar{p}$ as in other J/ψ radiative decays), the nonobservation of $X(p\bar{p})$ in $\omega p\bar{p}$ disfavors the pure FSI interpretation for the $p\bar{p}$ threshold enhancement in the decay $J/\psi \to \gamma p\bar{p}$.

ACKNOWLEDGMENTS

The BESIII Collaboration thanks the staff of BEPCII and the computing center for their hard efforts. This work is supported in part by the Ministry of Science and Technology of China under Contract No. 2009CB825200; National Natural Science Foundation of China (NSFC) under Contracts No. 10625524, No. 10821063, No. 10825524, No. 10835001, No. 10935007, No. 11125525, No. 11235011; Joint Funds of the National Natural Science Foundation of China under Contracts No. 11079008, No. 11179007; the Chinese Academy of Sciences (CAS) Large-Scale Scientific Facility Program; CAS under Contracts No. KJCX2-YW-N29, No. KJCX2-YW-N45; 100 Talents Program of CAS; German Research Foundation DFG under Contract No. Collaborative Research Center CRC-1044; Istituto Nazionale di Fisica Nucleare, Italy; Ministry of Development of Turkey under Contract No. DPT2006K-120470; U.S. Department of Energy under Contracts No. DE-FG02-04ER41291, No. DE-FG02-05ER41374, No. DE-FG02-94ER40823; U.S. National Science Foundation; University of Groningen (RuG) and the Helmholtzzentrum fuer Schwerionenforschung GmbH (GSI), Darmstadt; and WCU Program of National Research Foundation of Korea under Contract No. R32-2008-000-10155-0.

[1] J. Z. Bai *et al.* (BES Collaboration), Phys. Rev. Lett. **91**, 022001 (2003).
[2] M. Ablikim *et al.* (BESIII Collaboration), Chinese Phys. C **34**, 421 (2010).
[3] M. Ablikim *et al.* (BESIII Collaboration), Phys. Rev. Lett. **108**, 112003 (2012).
[4] J. P. Alexander *et al.* (CLEO Collaboration), Phys. Rev. D **82**, 092001 (2010).
[5] S. A. Athar *et al.* (CLEO Collaboration), Phys. Rev. D **73**, 032001 (2006).
[6] M. Ablikim *et al.* (BES Collaboration), Eur. Phys. J. C **53**, 15 (2008).
[7] M. Ablikim *et al.* (BES Collaboration), Phys. Rev. Lett. **99**, 011802 (2007).
[8] For a review, see S. Jin, Int. J. Mod. Phys. A **20**, 5145 (2005).
[9] A. Datta and P. J. O'Donnel, Phys. Lett. B **567**, 273 (2003).
[10] M. L. Yan, S. Li, B. Wu, and B. Q. Ma, Phys. Rev. D **72**, 034027 (2005).
[11] S. L. Zhu, Int. J. Mod. Phys. A **20**, 1548 (2005).
[12] M. Abud, F. Buccella, and F. Tramontano, Phys. Rev. D **81**, 074018 (2010).
[13] B. S. Zou and H. C. Chiang, Phys. Rev. D **69**, 034004 (2004).

[14] A. Sibirtsev, J. Haidenbauer, S. Krewald, U. Meissner, and A. W. Thomas, Phys. Rev. D **71**, 054010 (2005).
[15] D. V. Bugg, Phys. Lett. B **598**, 8 (2004).
[16] For a review, see C. S. Gao and S. L. Zhu, Commun. Theor. Phys. **42**, 844 (2004); E. Klempt and A. Zaitsev, Phys. Rep. **454**, 1 (2007).
[17] K. Abe *et al.* (BELLE Collaboration), Phys. Rev. Lett. **94**, 182002 (2005).
[18] B. Aubert *et al.* (*BABAR* Collaboration), Phys. Rev. D **74**, 051101 (2006).
[19] M. Ablikim *et al.* (BES Collaboration), Phys. Rev. Lett. **95**, 262001 (2005); **106**, 072002 (2011).
[20] M. Ablikim *et al.* (BESIII Collaboration), Chinese Phys. C **36**, 915 (2012).
[21] M. Ablikim *et al.* (BES Collaboration), Nucl. Instrum. Methods Phys. Res., Sect. A **614**, 345 (2010).
[22] J. Z. Bai *et al.* (BES Collaboration), Nucl. Instrum. Methods Phys. Res., Sect. A **344**, 319 (1994); **458**, 627 (2001).
[23] D. M. Asner *et al.*, Int. J. Mod. Phys. A **24**, 499 (2009).
[24] Z. Y. Deng *et al.*, High Energy Phys. Nucl. Phys. **30**, 371 (2006).
[25] S. Jadach, B. F. L. Ward, and Z. Was, Comput. Phys. Commun. **130**, 260 (2000); Phys. Rev. D **63**, 113009 (2001).
[26] R. G. Ping, Chinese Phys. C **32**, 599 (2008); D. J. Lange, Nucl. Instrum. Methods Phys. Res., Sect. A **462**, 152 (2001).
[27] J. Beringer *et al.* (Particle Data Group), Phys. Rev. D **86**, 010001 (2012).
[28] J. C. Chen, G. S. Huang, X. R. Qi, D. H. Zhang, and Y. S. Zhu, Phys. Rev. D **62**, 034003 (2000).
[29] W. D. Li, H. M. Liu *et al.*, in *Proceeding of CHEP06, Mumbai, India, 2006*, edited by Sunanda Banerjee (Tata Institute of Fundamental Research, Mumbai, 2006).
[30] W. Verkerke and D. Pirkby, eConf C0303241, MOLT007 (2003).
[31] M. Ablikim *et al.* (BESIII Collaboration), Phys. Rev. D **83**, 112005 (2011).
[32] M. Ablikim *et al.* (BESIII Collaboration), Phys. Rev. D **81**, 052005 (2010).
[33] M. Ablikim *et al.* (BESIII Collaboration), Phys. Rev. Lett. **104**, 132002 (2010).